Low-Aspect-Ratio Wings for Wing-Ships

Antonino Filippone* and Michael S. Selig†
Department of Aeronautical & Astronautical Engineering
University of Illinois at Urbana–Champaign
Urbana, IL 61801-2935

Abstract

Flying in ground poses technical and aerodynamical challenges. The requirements for compactness, efficiency, manouverability, off-design operation, open new areas of investigations in the field of aerodynamic analysis and design. A review of the characteristics of low-aspect ratio wings, in and out-of-ground, is presented. It is shown that the performance of such wings is generally inferior to that of slender wings, although in ground placement can yield substantial improvements in the aerodynamic efficiency. The use of tip devices, such as winglets and endplates, or an appropirate tip design, can change substantially the characteristics of the wing. Thin and thick airfoil sections are designed in ground effect, by using a multipoint inverse design method based on conformal mapping, to perform best either at constant lift or at increasing ground clearance. Three-dimensional computations have been performed with a panel code (VSAERO), and compared with available experimental data at aspect-ratios as low as 1. Wings of aspect-ratio 1.5 to 2.5 having the airfoil sections presented in this work have been computed at various ground clearances. It is concluded that design in ground effect is possible, and that the existing computational methods are adequate for an approximate study of low-aspect-ratio wings, although many flow phenomena require detailed investigastions.

*Post-doctoral Fellow, Member AIAA.

†Assistant Professor, Senior Member AIAA.

Introduction

Wing-in-ground planes (wing-ships) are aircraft that fly in near-ground. Since the lift is generated by forward flight, the wing-ship is fundamentally different from a hover-craft, which generates a jet of high pressure flow to lift itself. Due to the relatively low resistance of the air (1/800th of that of the water), the wing-ship can fly at a much higher speed than any existing ship. Experiences made in the former Soviet Union showed that the vehicles traveled fast, reliably, and were insensitive to rough seas.

Although ideas about hybrid ship-planes go back over a hundred years, the earliest practical designs were developed in the Soviet Union in the 1960s[1]. Some of the most outstanding vehicles are listed in Table 1. The prototypes were designed for military purposes, rescue operations, civil transport, and cargo services. One of the first commercial vehicles was the KM model (*Korabl Maket*, ship model), developed at the Central Hydrofoil Design Bureau at Gorkii in the early 1960s. It flew over the Caspian Sea at a top speed of 500 km/h powered by 10 jet engines. The A-90 Orlyonok wing-ship, designed in 1979 at Gorkii, could operate at a sea State 5, travel up beach and over flat terrain. The *Lun' Spasatel*, a later model derived from the KM in the late 1980s, had a larger wing span and a shorter fuselage. It was propelled by 8 jet engines, and had a cruise height of 1–4 meters above calm sea, although it could fly in 3.5 m high waves! The cruise height of other (less famous) Soviet wing-ships varied from 4 to 90 m on snow-bound terrain, flat tundra, and ocean seas. The construction of such vehicles was generally preceded by

Data	Korabl Maket	Lun Spasatel	Orlyonok A90	Beriev VVA-14	Raketa 2-2
wing-span (m)	32–40	44	31	—	19.5
total length (m)	93–106	73	58	—	33.5
loaded weight (t)	500	400	125–140	—	31
speed (Km/h)	400–500	450	350–400	—	180
max range (Km)	3000	3000	1100-3000	8000	500
cruise height (m)	—	1–4	—	—	—

Table 1: *Various dimensions of existing Soviet wing-ships. Ranges given in each box are dependent on the vehicle's version (commercial, military, cargo). Weights are intended for loaded vehicles. Some data are unknown.*

experimentation on smaller ones, single- or double-seaters, although a large vehicle weighing nearly 1000 tons (Beriev VVA-14) was designed and tested in 1976.

In the late 1980s it was estimated[2] that with improved aerodynamics a wing-ship weighing 300 tons would have a chord of 36 m, a wing span of 40 m, a total fuselage length of about 100 m, and would fly in ground effect at a cruise height of 3.5–7.0 m. Cruise speed would be about 250 km/h, and the vehicle would require 40,000 kW thrust from the propulsion system. Such a vehicle could operate year-around over 90% of the world seas, in particular: inland waters and offshore areas (life boats, coast guard units, high speed ferries), coastal traffic (as fast passenger ferries and freight), and overland (crossing flat areas, ice and snow, along with possible mono-rail vehicles). Other advantages include: reduced fuel consumption, high payload, high degree of comfort, easy to pilot, and low take-off speed. The low power required by this type of craft is a result of improved lift/drag ratio of a wing-in-ground effect as compared with flight out of ground effect.

More recently wing ships have been designed and produced in Germany, China and USA. These are generally much smaller units, often prototypes, with limited passenger capabilities. A preliminary design of a wing-in-ground aircraft was performed at the University of Illinois in 1993[3]. A critical analysis of wing-ship conceptual design is presented in[4].

The experience briefly reported above has led to the introduction of wings of various planforms (trapezoidal, rectangular, tapered, with/without dihedral) and the most disparate configurations.

The KM vehicle had rectangular wings mounted high, no dihedral, tail-wing tapered, swept, with large dihedral angle. The Lun' Spasatel had rectangular wing mounted low. The Orlyonok had wing mounted lower, small tip skegs, trailing edge flaps. Tapered and swept tail-plane with zero dihedral and four elevetors/side. Raketa 2-2 had small canards, down-turned tips, rectangular main wings with wing skegs, wing flaps, elevons, aspect-ratio about 1. The Beriev VVA-14 had short anhedral wings.

Wing-ships operate on the principle that by flying in close proximity to the ground the induced drag is reduced for a given lift coefficient because the downwash is inhibited by physical bounds. Ground effect become significant at cruise altitudes of $h/c \sim 0.1$–0.3. Assuming a design ground clearance of $h/c = 0.25$ with a design cruise height of 3–4 m, the wing chord becomes 12–15 m. To maintain a compact shape, a wing-ship must have a relatively short semi-span. The required lift, on the other hand, can be achieved by increasing the wing chord, which — at constant ground clearance — improves the ground effect gains. There sometimes appears to be a lower limit for h/c of approximately 0.1 below which the wing experiences a downforce termed *suck-down*. The effect depends on the geometry (in particular, on the amount of camber), and must be seriously investigated, to avoid the sinking effect on the ship. The concept of ***sinking*** a wing is widely applied in race car aerodynamics to increase the grip and the cornering speed of the car. The phenomenon is caused by a Venturi-type flow, where the acceleration below the wing leads to a pressure drop, that is enhanced as the ground clearance decreases.

Low-aspect-ratio wings, while best suited for the

present applications, are not well suited for conventional aircraft transport, since the efficiency L/D of the wing increases with the aspect-ratio. Therefore, the wing-ship performance must be compared to that an air-cushion machine (hover-craft) flying over water, rather than an aircraft.

The aim of this paper is to investigate the performance of ground effect performances of low aspect-ratio wings suited for wing-ship applications. Although high lift devices are sometimes an integral part of a wing-ship, high lift devices (e.g. flaps) are not addressed in this paper.

Low Aspect-Ratio Wings: A Review

Aerodynamic flows past low aspect-ratio wings are strongly three-dimensional and vorticity-dominated, with some degree of trailing-edge separation. In some cases the tip vortices can interact with each other downstream; whereas, on the wing itself the tip flow can reach the symmetry plane.

Low sweep is required to fly at high lift and slow speeds. In fact, low-$\mathcal{A}$ wings have a high angle of attack at $C_{L_{max}}$, a low lift-curve slope, and (generally) a longitudinal stability that deteriorates with the increasing angle of attack and moderate to high sweep angles. Sweepback causes the load on the wing of a given $\mathcal{A}$ to be further concentrated outboard when the increasing sweep angle. This promotes undesirable tip stall.

Experimental investigations on highly swept wing showed that the root sections do not experience high leading-edge pressure peaks[5]. In addition, the spanwise pressure gradients cause an outward drain of the boundary layer from the root sections. The combined influence of these two effects makes the root sections highly resistant to flow separation and therefore capable of developing local lift coefficients that more than compensate for the lift losses that occur when the tip sections of the wing stall. As a consequence, the wing root sections stall at very high angles, and the tip sections stall at much smaller angles. The thinner the wing, the lower the angle of attack at which the vortex flow is observed[5].

A combination of partial and progressive separation may cause destabilizing changes in the pitching moment, frequently at low values of C_L and in both incompressible and compressible flow[6]. This behavior is known as breakdown in the pitching moment, and the lift obtained at that point is the inflection lift.

Experiments carried out in Germany in the 1940s[7] for swept and unswept wings of aspect-ratios $\mathcal{A} = 1$–5 at $Re = 10^6$ showed that the $C_{L_{max}}$ is relatively insensitive to $\mathcal{A}$ for $\mathcal{A} > 2$, with an almost constant angle of maximum lift.

For smaller aspect-ratios ($1 < \mathcal{A} < 2$) the angle of maximum lift moves upwards to 30 deg. At even smaller aspect-ratios ($\mathcal{A} < 1$) experimental investigations[8] show that the values of the lift coefficient are considerably larger than those predicted by linear wing theory. The lift coefficient grows at a faster rate because the tip vortices strongly interact with each other, while the center of the wake is pushed downwards. Some nonlinear lifting line theory computations[8–12] are remarkably close to the measurements for both delta wings and swept-back wings with $\mathcal{A} = 1$. Experimental data for squared wings ($\mathcal{A} = 1$) report 'maximum lift coefficients that are extraordinarily high'[11] ($C_{Lmax} \sim 1.3$).

Another important detail is the leading-edge design, especially for swept-back wings. Sharp leading edges promote early flow separation (as with the delta wing) even at small angles of attack. An empirical correlation yielding the limiting leading-edge radius is given in[5], deduced from the analysis of a large number of wings.

The effect of aspect-ratio on lift and drag have been compared by Betz and Wieselsberger[12] using the Lanchester-Prandtl correlation, given by

$$C_D = C_{D_o} + \frac{C_L}{\pi}\left(\frac{1}{\mathcal{A}} - \frac{1}{\mathcal{A}_o}\right), \qquad (1)$$

where the index 'o' is relative to the reference data. The above expression was originally obtained for a lifting surface with elliptic spanwise loading. With Eq. 1 measured polars can be transformed to a known polar of given aspect-ratio. For wings in ground effect, such a correlation does not exist. The wing aspect-ratio influences the lift curve slope

according to $C_L'/C_{L_\infty}' = \mathcal{A}/(\mathcal{A}+2)$. The total drag of a wing consists of both the profile (viscous) drag and induced drag. The profile drag is largely independent from $\mathcal{A}$. The induced drag is created by the downwash generated by the tip vortices. Low-$\mathcal{A}$ wings have generally higher induced drag than slender wings.

Rolling moment due to sideslip of rectangular wings is considerably lower than that for delta wings and swept-back wings. For aspect-ratios in the range $2 < \mathcal{A} < 3$ experimental results show an increase for the decreasing aspect-ratios (NACA measurements[13]). The response of rectangular wings, delta wings and wings with sweptback to yawing moment due to sideslip is similar to that of rolling moment.

Tip Effects

Only few of the studies mentioned above has addressed the influence of the tip flows on the overall performances of the low aspect-ratio wings. In fact, as the wing becomes shorter, the geometry of the tip becomes essential in determining the aerodynamic characteristics. Round tips and fairings increase the effective aspect-ratio, promote or delay tip stall, and contribute in considerable amount to the total lift and drag forces. Tip separation occurs before than the wing trailing edge. The way separation occurs is strongly dependent on the geometry.

Vertical winglets/endplates are useful in improving the L/D ratio. The tip design should be a compromise between the extra vortex lift obtainable from a low-$\mathcal{A}$ wing and its lateral and longitudinal stability.

Earlier Experimental Work

There are several publications reporting experiments on low aspect-ratio wings. Ref[14] deals with aspect-ratio 1 wings, untwisted, unswept, 11- and 22%-thick, with flat tip or lower winglet, at various ground clearances. Experimental data for 11%-thick wing with winglet obtained by Carter[14] and Paulson-Kjelgaard[15] do not agree. Aspect-ratio 1 to 6, untwisted wings, with/without winglets at various ground clearances have been treated by Fink and Lastinger[16]. Aspect-ratio 2 (or higher) wing, untwisted, at various sweep angles, 18%-thick, round tip, with without flaps and elevons, and fuselage (wing-body combination) have been tested by Paulson and Kjelgaard[15]. Aspect-ratio 5 wing, untwisted, unswept, 12% thick, without other devices, out-of-ground effect[17]. High lift systems and short aspect-ratio wings in ground effect have been tested more recently at Göttingen[18]. Furthermore, there is a large body of experimental work from Lockeed[19] and Douglas Aircraft[20]. Other experimental data for low aspect-ratio wings are available in some older literature[21–22].

Airfoil Requirements

For this study, two airfoils were designed using the multipoint inverse method for multi-element airfoil design documented in[23]. This design method is driven by a MATLAB-based graphical user interface (GUI) enabling rapid, interactive design. The method couples an isolated-airfoil inverse design code documented in[24–25] with a panel method for multi-element airfoil analysis. In the current design problem, the single-element airfoil in ground effect is modeled as a two-element airfoil — the actual airfoil and its image due to the presence of the ground.

The two airfoils design here are referred to as "thin" and "thick" with design requirements listed in Table 2. The objective in setting the requirements was to study the effects of the operational lift range — low lift for the thin airfoil, high lift for the thick airfoil. The indicated nondimensional chord $\bar{c}$ is a measure of the resulting chord required for a wing in ground effect ship such that the take-off gross weight remains constant which nominally scales with $\bar{c}C_l$. The thickness requirement was dictated by assuming a constant span loading, and hence a desired constant physical wing thickness. The h'/c ratio was determined by the requirement of operating in the same sea state, e.g. constant height h' — as measured from the lowest point of the airfoil, in this case the trailing edge. Since h' is a constant in the design while the chord changes,

the h'/c changes accordingly.

Parameter	Thin	Thick
$C_{l,design}$	1 0	2
$\bar{c}$	1	0.5
$\bar{c}C_l \sim L$	1	1
t/c	6	12
h'/c	0.12	0.24
α (deg)	3.1	6.0

Table 2: *Thin and thick airfoil design requirements and resulting design angle of attack.*

The resulting airfoils at the required angles of attack are plotted to the design chord lengths (Table 2) in Fig. 1.

The effects on the lift coefficient of operating in ground effect as shown in Fig. for both the thin and thick airfoils. For the thin airfoil, the angles of attack of 4.5, 6.5, and 8.5 deg correspond to out-of-ground effect lift coefficients of 0.938, 1.167, and 1.393, while for the thick airfoil 4, 6, and 8 deg correspond to lift coefficients of 2.316, 2.546 and 2.772, respectively. What is clear from Fig.2 is that the thin and thick airfoils behave differently close in ground effect, while for h/c's values greater than approximately 2 a trend emerges. It should be noted that h/c is measured from the 1/4 chord point, and the airfoil rotates about this point on the chord line.

Some understanding of the changes in lift with proximity to ground can be gleaned from the velocity distributions about the thin airfoil at ground heights h/c of 0.25, 0.75, and ∞ for $\alpha = 6.5$ deg as shown in Fig. 3a. As the airfoil approaches the ground from ∞, the first effect on the airfoil is that due to the image vortex, in particular the "forward-wash" on the airfoil produced by the image-airfoil bound vortex. Thus, the "freestream" seen by the airfoil is effectively reduced, resulting in a reduced lift coefficient as ground is first approached. This reduction in the "freestream" is the cause for the overall lower velocity distribution about the thin airfoil for $h/c = 0.75$ in Fig. 3a as compared with the out-of-ground effect case. As the airfoil moves closer to the ground, the "forward-wash" effect increases as can be seen by a lowering of the upper surface velocity (non-dimensionalized still be V_∞). A stronger effect — the ram effect — dominates, however. The lower surface flow is brought much closer to stagnation, and consequently this larger effect combined with the image vortex effect leads to a net increase in lift as shown Fig. 2. The dominant ram effect for the lower ground heights is driven mainly by the angle of attack of the airfoil, resulting in slowing of the flow beneath the airfoil — the higher the angle, the greater the ram-effect contribution to lift for a given ground height.

For the thick airfoil, the lift close to the ground as indicated in Fig. 2 does not rise as it did with the thin airfoil for two reasons. First, the image vortex effect dominates largely as a result of the higher lift coefficients of the thick airfoil. This effect dominates the velocity distributions shown in Fig. 3b for an angle of attack of 6 deg for h/c of 0.25, 0.75, and ∞. Second, the ram effect is not as large because the angle for a given lift coefficient is not as great as it is for the thin airfoil.

Another ground effect not appreciably displayed in these results for lifting airfoils is the venturi effect. This latter effect is present with inverted airfoils, such as those employed in auto racing, e.g. Indy cars. In this case, the flow is greatly accelerated between the airfoil in the ground resulting in a suck-down effect, or in motorsports terminology, downforce. Also, the "forward-wash" effect becomes a "rear-wash" leading to a locally higher freestream and hence greater downforce.

The effect of the ground on the maximum lift coefficients of the thin and thick airfoils can be deduced from the velocity distributions shown in Figs. 4a and 4b, which correspond to respective constant lift coefficients, rather than constant angles of attack as in Fig. 3a and Fig. 3b. For the thin airfoil since the lift at $h/c = 0.75$ is less than that out-of-ground effect (Fig. 2), the angle of attack must increase for this height. For $h/c = 0.25$, however, the gain in lift with ground proximity leads to a lowering of the angle of attack. In particular, the constant lift coefficient of 1.167 yielded corresponding angles of attack of 6.5, 6.83, and 5.45 deg for h/c values of ∞, 0.75 and 0.25 respectively. As can be seen, while the angle of attack is less near the ground ($h/c = 0.25$), the suction-side pressure gradient on the airfoil changes very little. Thus, it can be expected that for this airfoil the maximum

lift coefficient is hardly changed by ground effect.

For the thick high-lift airfoil, however, the trends are reversed. To compensate for the dramatic loss in lift, the angle of attack must be increased substantially. Specifically, to maintain the constant lift coefficient of 2.186, angles of attack of 2.9, 6.4 and 12 deg were required for h/c values of ∞, 0.75 and 0.25 respectively. From Fig. 4b it can be seen that the high angle of attack in ground effect leads to a strong adverse pressure gradient on the leading-edge upper surface. When this is compared with the out-of-ground effect case, it can be deduced that the out-of-ground effect maximum lift coefficient will be greater than that in ground effect. Thus, the maximum lift characteristics of airfoils in ground effect as compare with the out-of-ground effect conditions depends strongly on the airfoil geometry — the maximum lift coefficient of highly cambered airfoils will decrease with decreasing ground clearance owing to the occurrence of a strong leading-edge suction peak.

The Low Aspect-Ratio Wings

Methods used to predict the performance of wings in ground range from 2-D potential flow methods, with/without boundary layer displacement effects[18], to 3-D steady/unsteady lifting surface method[26]. Approximated linear methods, such that of Multhopp[9], Betz[11] and Truckenbrodt[17] are sometimes used for wings with moderate sweeps.

In the present work the low-order panel method VSAERO[27-28] has been used for the calculations shown in this paper. Currently, problems described by several hundred body and wake panels require no more than a few minutes per run on a personal computer. The low computing cost makes VSAERO a practical tool for solving complex non-linear aerodynamic problems. An interface is provided to VSAERO to compute entire polar characteristics of a given wing. This computer code has been validated in the present work by computing low-aspect ratio wings in- and out of ground. The results have been compared with experimental data.

Figure 5 shows the results for the computed polar of an aspect-ratio $\mathcal{A} = 5$ wing having a constaint airfoil section NACA 2412. The computed data are compared with experiments with a wing out of ground. The computation was performed by using a free wake analysis and a boundary layer iteration, that works very well under mild pressure gradients. The computed polar is very close to the experimental data for a wide range of angles of attack.

Wings of aspect-ratio as low as one, Fig. 6, have been computed both in- and out of ground effect, after the wake separation line has been adjusted. The results are generally satisfactory, although problems of tip flow separation are very difficult to handle. Also the results of Fig. 7 have been obtained with a free wake analysis and a boundary layer interaction.

Figure 8 shows the computed C_L and the efficiency C_L/C_D versus aspect-ratio for the two wings at $\alpha = 0$ at the design ground clearances. The values obtained for the thick wing are considerably higher.

The lift characteristics of two wings, having the thin and the thick airfoil sections, respectively, have been computed as shown in Fig. 9. The thin wing was at the design clearance of $h/c = 0.12$, has an aspect-ratio $\mathcal{A} = 2.0$, with a unit chord (design conditions of Table 2), while the thick wing was placed at the design clearance $h/c = 0.24$, had the same span, but half the chord, hence an aspect-ratio $\mathcal{A} = 4.0$. The lift values of the thick wing are much larger, showing a gap ΔC_L of about 0.75 in ground effect.

With the airfoils section described in this paper we have computed rectangular wings of aspect-ratios $\mathcal{A} = 1.5, 2.0, 2.5$, at the design ground clearances $h/c = 0.12$, 0.24 and out of ground, with round tips and endplates. Figure. 8a shows the lift characteristics for the thin wing, Fig8b shows the corresponding aerodynamic efficiency C_L/C_D. The angle of attack was $\alpha = 0.0$. The values obtained for a wing with a rectangular endplate are considerably higher than the values obtained wih a simple round tip. The ffect of the plate is to diffure the tip vortex and reduce the loss of lift at the outer board. The effect of the spanwise lift distribution is shown in Fig. , at ground clearance $h/c = 0.12$ and out of ground.

Conclusions

It is possible to design airfoils in ground effect, using multi-point design techniques, that include geometrical constraints and specified pressure distribution. The method features the possibility of designing an airfoil with a flap system (also in ground effect).

The inverse design method is very useful to analyze finite wings (an inverse design method for finite wings in ground effect does not exist). The analysis has been carried out with a three-dimensional panel method, for both simple wings and wings with tip devices (endplates).

For the airfoil in ground effect is was found that the airfoil loses lift (with respect to an airfoil out of ground) at high lift, and gains lift at low lift. This is due to the negative effect of the mirror image airfoil with the airfoil itself is highly loaded. Negative ground effects have been found on cambered airfoils in ground placement.

The lift curve slope increases in ground effect for both the thin and thick wing. At some negative angles of attack there is an inversion in the lift generated, since the wing-in-ground becomes less effective than the wing out of ground.

Low aspect-ratio wings in ground effect have been computed with a three-dimensional panel method (VSAERO). The results have been compared with experimental data. At relatively high aspect-ratios ($\mathcal{A} \sim 5$) the results are encouraging, both in- and out of ground. At lower aspect ratios tip separation occurs. If the separation line is known, the results are in excellent agreement with the experimental data for aspect ratios as low as 1 (squared wings).

The wing C_L increases slightly with the increasing aspect-ratio, and shows values sensibly higher for the thick wing. The lift coefficients are in both cases much lower than the values computed for the 2D airfoils in the design stage. This is clearly due to the three dimensional effects.

The thick wing has also a larger aerodynamic efficiency, both in- and out-of-ground. At the aspect-ratios considered the thick wing is about three times as efficient.

Three-dimensional effects on the lift can be reduced by using endplates of appropriate shape and size. Computations performed on the thin wing at all aspect-ratios, in and out-of-ground effect, have shown a substantial reduction in the loss of lift due to end-effects, and tip vortex roll-up. Other technical solutions may include boundary layer fences to reduce the three-dimensionality of the flow.

The nature of the tip geometry is essential in determining the characteristics of the wings of low aspect-ratio. It is not possible to compute flow separation with inviscid methods; however, separation affects the wing characteristics in a stronger degree than in slender wings.

Main problems are believed to be the tip effects (which can change consistently the wing characteristics, in and out of ground), the stability of the wing, both static and dynamic, the take-off conditions, and the behavior during banking flight.

Acknowledgements

The authors with to thank Ashok Gopalarathnam for his help in developing the MATLAB-GUI interface used extensively in the airfoil design part of this effort.

References

[1]B. Gurton. *The Encyclopedia of Russian Aircraft 1875-1995*, pages 511–526. Motorbooks International Publishers & Wholesalers, Osceola, WI 54020, USA, 1995.

[2]R. Di Trillo, editor. *Jane's High-Speed Marine Craft and Air-Cushion Vehicles.* Jane's Tranport Data, 1989.

[3]F.A. Balow III, J.G. Guglielmo, and K.R. Sivier. Design and Evaluation of a Midsize Wing-in-Ground Effect Transport. *AIAA Paper 93-3952*, 1993.

[4]S. Ando. Critical Review of Design Philosophies for Recent Transport WIG Effect Vehicles. *Trans. Japan Soc. Aero. Space Sci.*, Vol. 33, No. 99, pp. 31–40, 1990.

[5]C.G. Furlong and J.G. McHugh. A Summary and Analysis of the Low-Speed Longitudinal Characteristics of Swept Wings at High Reynolds Number. Report NACA 1339, 1957.

[6]J.C. Cooke and G.C. Brenner. *Boundary Layer and Flow Control*, The Nature of Separation and Its Prevention by Geometric Design in a Wholly Subsonic Flow, pages 144–185. Pergamon Press, Oxford, 1961.

[7]K. Bussmann and K. Kupfermann. Theoretische und experimentelle Untersuchngen an schiebenden Flügeln insbesondere Pfeil und Deltaflügeln. *ZWB Lufo. TB 11*, Vol. 8, pp. 245–251, 1944.

[8].K Gersten. Nichtlineare tragflächentheorie insbesondere für tragflügel mit kleinem Seitenverhältnis. *Ing-Arch*, Vol. 30, pp. 431–452, 1961.

[9]H. Multhopp. Methods for Calculating the Lift Distribution of Wings (Subsonic Lifting Surface Theory). Report ARC RM-2884, 1950/55.

[10]E. Truckenbrodt. Tragflächentheorie bei Inkompressibler Strömung. *Jb. WGL*, pp. 40–65, 1953.

[11]Betz. A. *Aerodynamic Theory*, Applied Airfoil Theory, Vol. 4, Division J. Pergamon Press, Oxford, 1934.

[12]C. Wieselberger. *Experimentelle Prüfung der Umrechnungsformeln.* Oldenbourg, Berlin-Munchen, 1921. in Prandtl, Wieselberger, and Betz : Ergebnisse der Aerodynamischen Versuchsanstalt zu Göttingen, Vol. 1, pp. 49-53.

[13]J. Fischel, R.L. Naeseth, J. Hagermn, and W.O. O'Hare. Effect of Aspect-Ratio on the Low Speed Characteristics of Low Aspect-Ratio Wings Equipped with Flap and Retractable Ailerons. Report NACA 1091, 1952. (formerly TN 2347, TN-2348).

[14]A.W. Carter. Effect of Ground Proximity of the Characteristics of Aspect-Ratio 1 Airfoils with and without Endplates. TN D-970, NACA, 1961.

[15]J.W. Paulson and Kjelgaard S.O. An Experimental and Theoretical Investigation of Thick Wings at Various Sweep Angles in and out of Ground Effect. Report NASA 2068, 1982.

[16]M.P. Fink and J.L. Lastinger. Aerodynamic Characteristics of Low-Aspect-Ratio Wings in Close Proximity to the Ground. TN D-926, NACA, 1961.

[17]H. Schlichting and E. Truckenbrodt. *Aerodynamics of the Airplane.* McGraw-Hill, New York, 1979.

[18]D. Steinbach and K. Jacob. Some Aerodynamic Considerations of Wings near Ground. *Trans. Japan Soc. Aero. Space Sci.*, Vol. 34, No. 104, pp. 56–70, Aug. 1991.

[19]Lockeed Company. Wind Tunnel Investigation of Single and Tandem Low Aspect-Ratio Wings in Ground Effect. Technical Report L-53, Lockeed Fluid Dynamics Laboratory, Calif., May 1963.

[20]Douglas Aircraft Co. Wing-in-Ground Effect Vehicles. Technical Report, 1977.

[21]L. Prandtl. Application of Modern Hydrodynamics to Aeronautics. NACA 116, 1921.

[22]I.H. Abbott and A.E. Von Doenhoff. *Theory of Wing Sections.* Dover Ed., New York, 1959.

[23]A. Gopalarathnam and M. Selig. A Multipoint Inverse Design Method for Multi-Exlement Airfoil Design. *J. Aircraft*, (to appear).

[24]Selig.M.S. and M.D. Maughmer. Generalized multipoint inverse airfoil design. *AIAA J.*, Vol. 30, No. 11, pp. 2618–2625, Nov. 1992.

[25]Selig.M.S. and M.D. Maughmer. Multipoint inverse airfoil design method based on conformal mapping. *AIAA J.*, Vol. 30, No. 5, pp. 1162–1170, May 1992.

[26]A.O. Nuhait and D.T. Mook. Numerical Simulation of Wings in Steady and Unsteady Ground Effects. *J. Aircraft*, Vol. 26, No. 12, pp. 1081–1089, Dec. 1989.

[27]B. Maskew. Prediction of Subsonic Aeorodynamic Characteristics: A Case for Low-Order Panel Methods. *J. Aircraft*, Vol. 19, No. 2, pp. 157–163, Feb. 1982.

[28]J. Nathman. *Vsaero User's Manual, Version V 5.6.* Analytical Methods Inc.

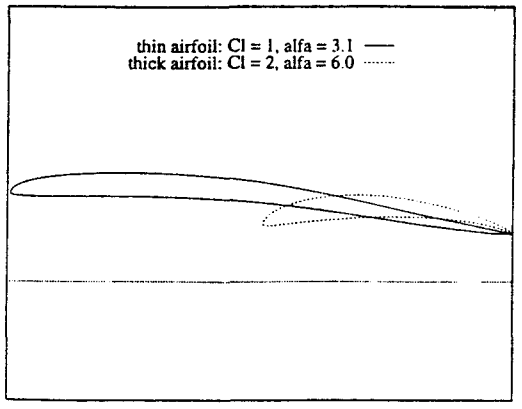

Figure 1. : Designed airfoils sections. Design points are: thin airfoil $C_L = 1.0$, $\alpha = 3.1$ deg, $h/c = 0.12$; thick airfoil: $C_L = 6.0$, $\alpha = 2.0$ deg, $h/c = 0.24$.

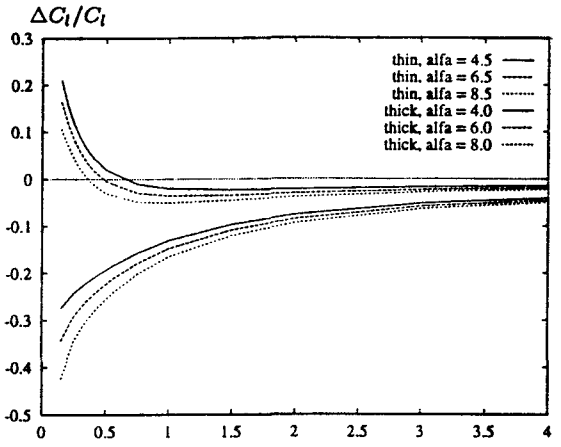

Figure 2. : Lift characteristics of the thin and thick airfoils as a function of the angle of attack and ground clearance.

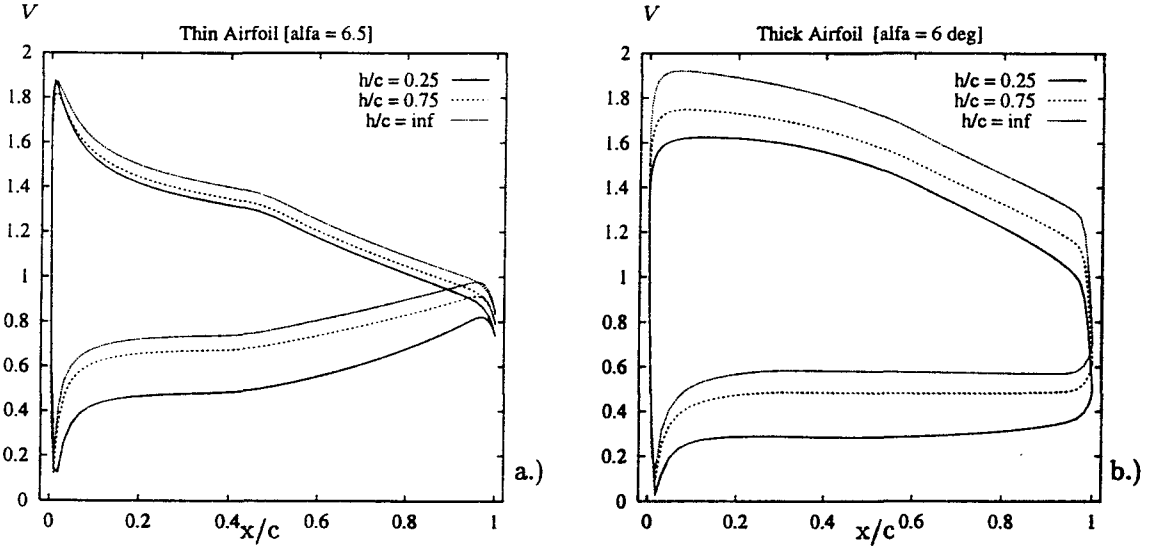

Figure 3. *Computed velocity distributions on the thin a.) and thick airfoil b.), as function of the ground clearance.*

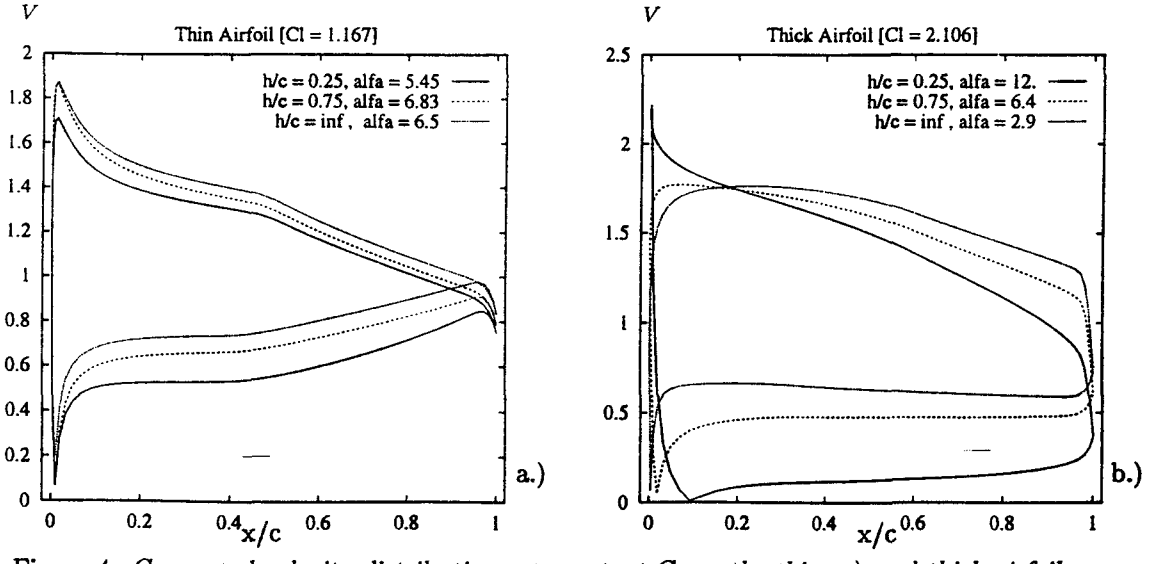

Figure 4. *Computed velocity distributions at constant C_l on the thin a.) and thick airfoil b.), as function of the ground clearance.*

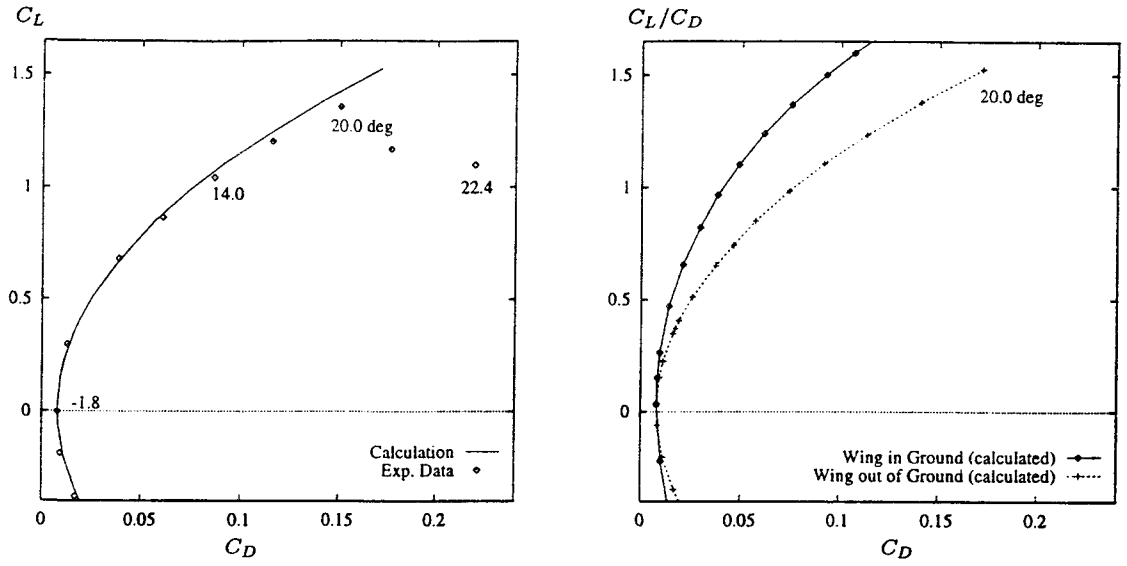

Figure 5. *Computed polar for a NACA 2412 wing with $\mathcal{A} = 5$ having a round tip. Graphic of the left shows comparison between the calculated polar and the experimental data. The graphic on the right shows a comparison of predictions between in- and out-of-ground effect for the same wing.*

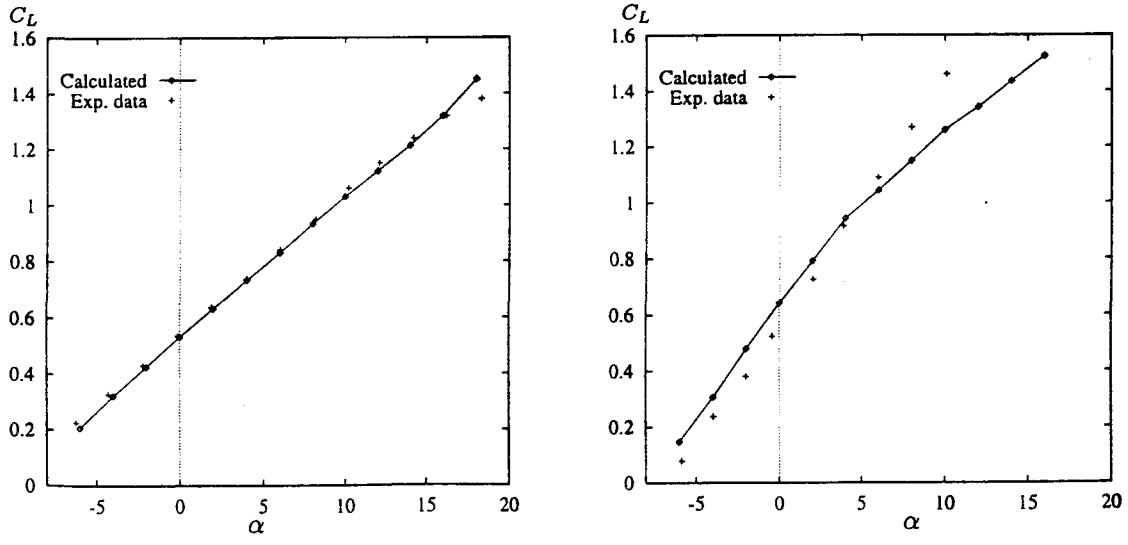

Figure 6. *Computed C_L-curve for a rectangular wing of aspect-ratio 2 with flat tip, Glen-Martin 22 airfoil section (22%-thick), out- and in-ground effect (left and right graphic, respectively). The present results are compared with the experimental data of Ref. 14.*

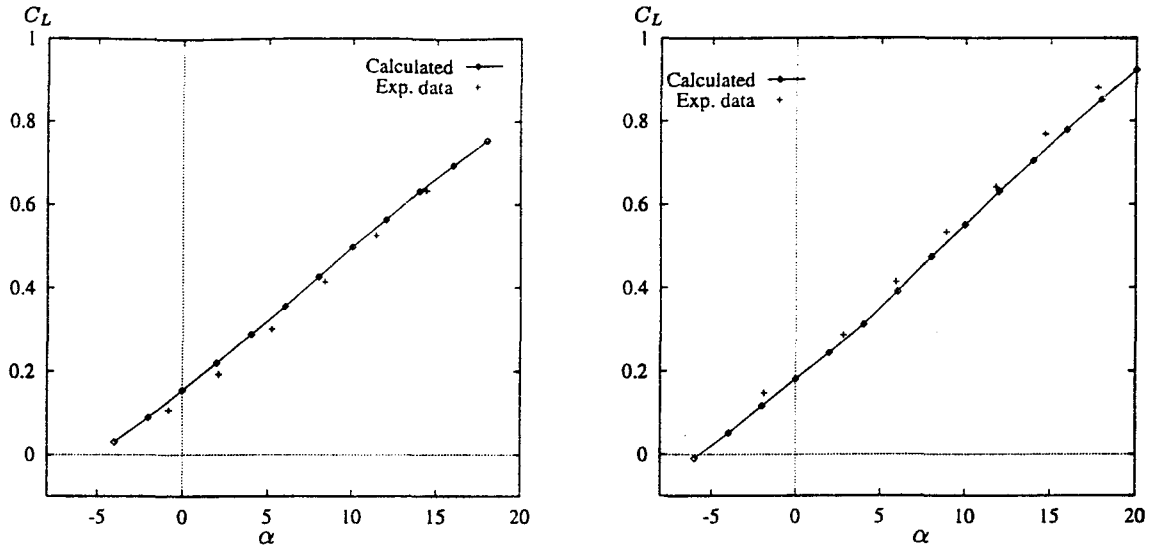

Figure 7. *Computed C_L-curve for a rectangular wing of aspect-ratio 1 with flat tip, Glen-Martin 11 airfoil section (11%-thick), out- and in-ground effect (left and right graphic, respectively). The present results are compared with the experimental data of Ref. 14.*

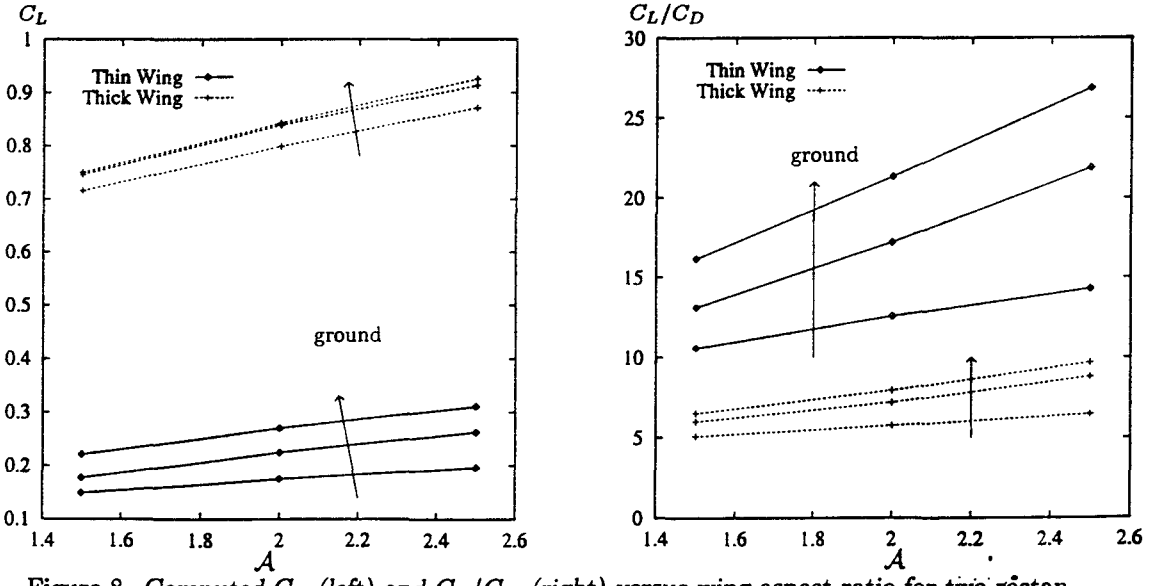

Figure 8. *Computed C_L (left) and C_L/C_D (right) versus wing aspect-ratio for two rectangular wings having round tip. Angle of attack $\alpha = 0$ deg. Ground clearances: $h/c = 0.12$, 0.24, and ∞.*

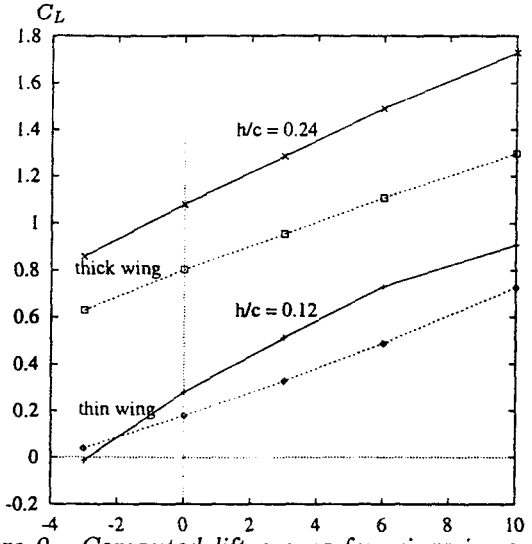

Figure 9.: Computed lift curves for wings in- and out-of-ground effect. Thick wing $\mathcal{A} = 4.0$ and $h/c = 0.24$; thin wing $\mathcal{A} = 2.0$ and $h/c = 0.12$.

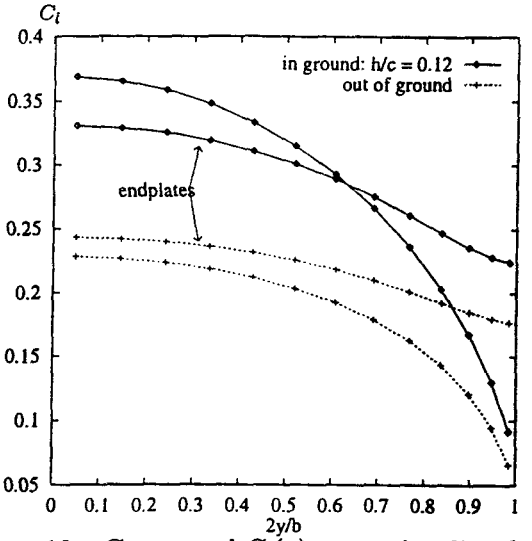

Figure 10.: Computed $C_l(s)$ spanwise distribution for a rectangular thin wing of aspect-ratio $\mathcal{A} = 1.5$ at $\alpha = 0$ deg, with round tip and endplate, in- and out-of-ground.

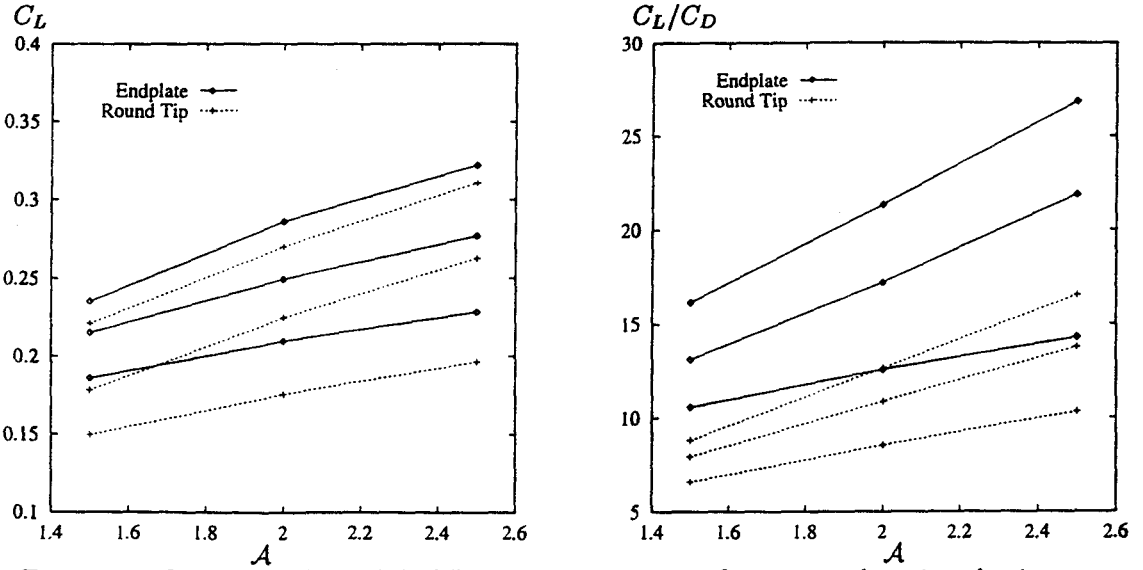

Figure 11. *Computed C_D and C_L/C_D versus aspect-ratio for rectangular wings having a thin airfoil section with and without endplates Ground clearances: $h/c = 0.12, 0.24, \infty$.*